Nozaki, Y., Reynolds, J. A., & Tanford, C. (1978) *Biochemistry 17*, 1239-1246.
Oldfield, E., Norton, R. S., & Allerhand, A. (1975) *J. Biol. Chem. 250*, 6368-6380.
Opella, S. J., Cross, T. A., DiVerdi, J. A., & Sturm, C. F. (1980) *Biophys. J. 32*, 531-548.
Reynolds, J. A., & Tanford, C. (1970) *Proc. Natl. Acad. Sci. U.S.A 66*, 1002-1007.
Robinson, N. C., & Tanford, C. (1975) *Biochemistry 14*, 369-378.
Shindo, H., Egan, W., & Cohen, J. S. (1978) *J. Biol. Chem. 253*, 6751-6755.
Smilowitz, H. (1974) *J. Virol. 13*, 94-99.
Smilowitz, H., Carson, J., & Robbins, P. W. (1972) *J. Supramol. Struct. 1*, 8-18.
Sugimoto, K., Sugisaki, H., & Takanami, M. (1977) *J. Mol. Biol. 110*, 487-507.
Valentine, K. G., Schneider, D. M., Leo, G. C., Colagno, L. A., & Opella, S. J. (1986) *Biophys. J. 49*, 38-40.
Williams, R. W., & Dunker, A. K. (1977) *J. Biol. Chem. 252*, 6253-6255.
Wilson, M. L., & Dahlquist, F. W. (1985) *Biochemistry 24*, 1920-1928.
Woolford, J. L., & Webster, R. E. (1975) *J. Biol. Chem. 250*, 4333-4339.

Backbone Dynamics of a Model Membrane Protein: Measurement of Individual Amide Hydrogen-Exchange Rates in Detergent-Solubilized M13 Coat Protein Using ^{13}C NMR Hydrogen/Deuterium Isotope Shifts†

Gillian D. Henry, Joel H. Weiner, and Brian D. Sykes*

Medical Research Council Group in Protein Structure and Function and Department of Biochemistry, University of Alberta, Edmonton, Alberta, T6G 2H7, Canada

Received December 19, 1986

ABSTRACT: Hydrogen-exchange rates have been measured for individual assigned amide protons in M13 coat protein, a 50-residue integral membrane protein, using a ^{13}C nuclear magnetic resonance (NMR) equilibrium isotope shift technique. The locations of the more rapidly exchanging amides have been determined. In D_2O solutions, a peptide carbonyl resonance undergoes a small upfield isotope shift (0.08–0.09 ppm) from its position in H_2O solutions; in 1:1 H_2O/D_2O mixtures, the carbonyl line shape is determined by the exchange rate at the adjacent nitrogen atom. M13 coat protein was labeled biosynthetically with ^{13}C at the peptide carbonyls of alanine, glycine, phenylalanine, proline, and lysine, and the exchange rates of 12 assigned amide protons in the hydrophilic regions were measured as a function of pH by using the isotope shift method. This equilibrium technique is sensitive to the more rapidly exchanging protons which are difficult to measure by classical exchange-out experiments. In proteins, structural factors, notably H bonding, can decrease the exchange rate of an amide proton by many orders of magnitude from that observed in the freely exposed amides of model peptides such as poly(DL-alanine). With corrections for sequence-related inductive effects [Molday, R. S., Englander, S. W., & Kallen, R. G. (1972) *Biochemistry 11*, 150–158], the retardation of amide exchange in sodium dodecyl sulfate solubilized coat protein has been calculated with respect to poly(DL-alanine). The most rapidly exchanging protons, which are retarded very little or not at all, are shown to occur at the N- and C-termini of the molecule. In the N-terminal region, up to and including aspartic acid-12, retardations no more than about 20-fold are observed; these exchange rates are much more rapid than the values determined for regions of stable secondary structure in other proteins. Proceeding inward from the C-terminus, by contrast, reveals a steep and progressive increase in retardation of the exchange rate from threonine-46 to leucine-41 in a manner suggestive of the fraying end of a helical segment. A model of the detergent-solubilized coat protein is constructed from these H-exchange data which is consistent with circular dichroism and other NMR results.

Measurement of the exchange rates of backbone amide protons in a protein has been recognized for many years to be a potential source of structural and dynamic information. The initial H-exchange experiments on model polypeptides (Linderstrom-Lang, 1955; Linderstrom-Lang & Schellman, 1959) in fact provided much of the initial impetus for the development of current concepts of conformational fluctuations in proteins. Although the interpretation of H-exchange data is still controversial (Woodward et al., 1982; Englander & Kallenbach, 1984), the rates of exchange of amide protons with the solvent are generally considered to be heavily influenced by H bonding, for example, amide exchange rates were recently used to corroborate the solution structure of the *lac* repressor head piece as determined by nuclear magnetic res-

† Supported by the Medical Research Council of Canada (MRC Group in Protein Structure and Function and MRC Grant MT5838) and the Alberta Heritage Foundation for Medical Research. Paper 2 in the series is by Henry et al. (1987).

* Address correspondence to this author at the Department of Biochemistry, University of Alberta.

0006-2960/87/0426-3626$01.50/0

onance (NMR)[1] techniques (Boelens et al., 1985). H-exchange experiments can also provide information on the conformational equilibria (i.e., folding and unfolding of a segment of polypeptide chain) which by necessity precede the exchange event (Roder et al., 1985).

Detailed interpretation of H-exchange data relies heavily on the resolution of individual amide protons which can be attributed to specific amino acids in the primary sequence. Recently, the application of two-dimensional ^1H NMR spectroscopy to proteins has led to greatly enhanced resolution and aided assignment of the amide proton region. The most notable example is the basic pancreatic trypsin inhibitor and its analogues (Wagner & Wuthrich, 1982a,b; Strop & Wuthrich, 1983; Wagner et al., 1984; Tuchsen & Woodward, 1985); other examples include apamin (Wemmer & Kallenbach, 1983; Dempsey, 1986), the *lac* repressor head piece (Boelens et al., 1985), the S-peptide of ribonuclease S (Kuwajima & Baldwin, 1983), the terminal helix of cytochrome *c* (Wand et al., 1985), and several adjacent protons from the F-helix of myoglobin (Vasent Kumar & Kallenbach, 1985). As a result, amide exchange rates are now known for a number of assigned protons in several small proteins. As an alternative to these more traditional proton-detected "exchange-out" experiments, in which the protonated protein gradually equilibrates with a vast excess of solvent D_2O, we have applied an indirect ^{13}C equilibrium approach (Feeney et al., 1974; Hawkes et al., 1978; Kainosho & Tsuji, 1982) to the measurement of H exchange in the detergent-solubilized coat protein of the filamentous coliphage M13. The biosynthetic incorporation of a number of ^{13}C-1 (carbonyl) labels into M13 coat protein and the assignment of the ^{13}C NMR spectra were described in the preceding paper (Henry et al., 1987). H-exchange rates have been determined for the amide proton of the adjacent amino acid from the line shape of the isotopically shifted carbonyl resonances in equimolar H_2O/D_2O solutions (Feeney et al., 1974). This method provides resolution, through the isotopically enriched carbon atoms, which is not readily obtainable in the ^1H spectrum of M13 coat protein (Cross et al., 1980); it also provides a method for measuring the most rapidly exchanging amide protons in a protein which are not normally accessible except perhaps at low pH values and low temperatures. Exchange rates, as a function of pH, have been determined for 12 individual assigned amide protons of SDS-solubilized M13 coat protein.

M13 coat protein is a 50-residue amphiphilic polypeptide with 2 charged hydrophilic domains flanking a 19-residue hydrophobic core (Asbeck et al., 1969; Nakashima & Konigsberg, 1974). The sequence is given in Figure 1 of the preceding paper (Henry et al., 1987). During the reproductive cycle of the phage, the coat protein exists alternately as an α-helical rod in the mature virus (Marvin, 1966; Marvin et al., 1974) and as an integral protein of less certain structure in the inner membrane of the host *Escherichia coli* cell (Smilowitz et al., 1972). The detergent-solubilized form of the protein, which was suggested to contain about 50% α-helix and 30% β-sheet from circular dichroism data, is considered to be a reasonable model of the membrane-bound form (Nozaki et al., 1976, 1978). The H-exchange results have been correlated with our previous quantitative (Henry et al., 1986) and qualitative (Henry et al., 1987) dynamic studies to produce a model for the protein–detergent complex.

[1] Abbreviations: NMR, nuclear magnetic resonance; SDS, sodium dodecyl sulfate; ppm, parts per million; $^2\Delta$, two-bond isotope shift; PDLA, poly(DL-alanine); Me_4Si, tetramethylsilane; τ, mean exchange lifetime; τ_c, overall rotational correlation time.

Experimental Procedures

Labeled phage and protein-containing SDS micelles were prepared as described in the preceding paper (Henry et al., 1987). Samples in 50% D_2O were concentrated to half their final volume and diluted with D_2O-containing buffer such that the final solution contained 10 mM SDS, 5 mM sodium borate, 90 mM sodium chloride, and 1:1 H_2O/D_2O by volume. The buffer concentration was kept to a minimum in order to maintain a constant ionic strength throughout the pH titration range. Samples prepared in H_2O contained 5–10% D_2O to provide a lock signal. The pH measurements are direct meter readings, uncorrected for the presence of D_2O. pH readings were taken both before and after collection of the NMR spectrum and always agreed to within at least 0.1 pH unit, even though the samples were not well buffered throughout the entire pH titration range.

^{13}C NMR spectra were recorded at 75.45 MHz on a Nicolet NT 300 WB spectrometer using MLEV16 decoupling (Levitt & Freeman, 1981). Typically, 8K data points were collected with a sweep width of ±2000 Hz, giving a spectral resolution of about 1 Hz. Chemical shifts are given relative to Me_4Si at 0 ppm and measured with respect to internal dioxane and 67.37 ppm (Shindo et al., 1978). Exchange rates were measured by fitting the spectra to simulated spectra generated by the Nicolet two-site exchange program NMRXCH. For curve fitting, the free induction decay was zero-filled to 16K data points and a 1–2-Hz line broadening applied. This is in contrast to Figures 1–5 which have been resolution enhanced. The isotope shift, $^2\Delta$, was determined by fitting simulated curves to spectra obtained at low pH.

Theory

Measurement of H-Exchange Rates. The ^{13}C resonance of a peptide carbonyl carbon undergoes a small two-bond upfield isotope shift ($^2\Delta$ = +0.08–0.09 ppm) upon deuteriation of the adjacent amide nitrogen atom [Feeney et al., 1974; see also Hansen (1983)]:

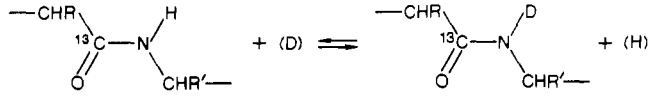

This corresponds to a shift of 6–7 Hz at a spectrometer frequency of 75 MHz. In a 1:1 H_2O/D_2O mixture, the line shape of the carbonyl resonance is determined by the rate of exchange of protein-bound protons or deuterons with those of the solvent. This situation is described by the classic two-site exchange equation of McConnell (1958). The dependence of line shape on exchange rate is determined by the frequency difference of the two forms in the absence of exchange, in this case, the shifts of the individual protonated and deuteriated species. In 1:1 H_2O/D_2O mixtures, two peaks are observed in the slow exchange limit [$\tau \gg 1/2\pi(^2\Delta)$] corresponding to ^{13}CONH (downfield) and ^{13}COND (upfield) (Feeney et al., 1974), where $^2\Delta$ is the isotope shift in hertz and τ is the mean lifetime, defined in terms of the individual lifetimes of the protonated and deuteriated forms (τ_H and τ_D, respectively):

$$\tau = \tau_H\tau_D/(\tau_H + \tau_D) \quad (1)$$

In the fast exchange limit [$\tau \ll 1/2\pi(^2\Delta)$], a single resonance is observed at an average chemical shift. It should be noted that the terms "fast" and "slow" as defined in the context of exchange lifetimes are operational definitions in terms of $2\pi(^2\Delta)$ (where $1/\tau = 2k_{ex} \simeq 40\ s^{-1}$) and do not necessarily comment on H-exchange rates on an absolute scale.

In between the slow and fast exchange limits, an intermediate series of spectra is observed. Within this window

(corresponding to an exchange rate $k_{ex} \simeq 2$–$125\ s^{-1}$), the line shape of the carbonyl carbon may be used to determine τ by comparing experimental spectra with computer simulations. This requres a knowledge of the line width in the absence of exchange, which was obtained from spectra acquired in water and/or in the slow exchange limit. It was assumed that the line widths of the protonated and deuteriated species were equal. It should be noted that the carbonyl carbon reflects exchange at the amide nitrogen of the succeeding residue, i.e., the carbonyl carbon of phenylalanine-11 reflects exchange at aspartic acid-12.

Hydrogen-exchange rates may be brought from the slow to the fast exchange limits (i.e., into the experimental "window") by adjusting either pH or temperature. Exchange is catalyzed by both H^+ and OH^- and is generally described by

$$k_{ex} = k_H[H^+] + k_{OH}[OH^-] \quad (2)$$

where k_H and k_{OH} are acid- and base-catalyzed rate constants. For model peptides, k_{OH} is about 6 orders of magnitude greater than k_H, resulting in a minimum H-exchange rate at pH $\simeq$3. Above pH $\simeq$4, the rate is proportional to $[OH^-]$ increasing 10-fold for each unit rise in pH [see Englander and Kallenbach (1984)]. All of the experiments described herein are on the base-catalyzed limb of the rate vs. pH curve. Assuming $\tau_H = \tau_D$, the exchange rate of an individual proton, k_{ex}, is given (from eq 1) as $k_{ex} = 1/2\tau$. This is equivalent to assuming that the populations of the protonated and deuteriated forms of the protein reflect the isotopic composition of the solvent; i.e., there is no equilibrium isotope effect. Such an isotope effect does exist (Hvidt & Nielsen, 1966; Englander & Poulsen, 1969; Englander et al., 1972), but it is small enough to be neglected. However, in the presence of only 50% H_2O, eq 2 becomes (in the base-catalyzed regime) $k_{ex} = k_{OH}[OH^-]_{measured}/2$; thus τ, the mean lifetime derived from spectral simulations, is given:

$$1/\tau = 2k_{ex} = k_{OH}[OH^-]_{measured} \quad (3)$$

where $[OH^-]_{measured}$ is the total concentration of OH^- and OD^- determined from the pH meter reading. As an alternative to line shape analysis using computer simulations, the exchange rate may be judged from the pH of coalescence of the two lines; the characteristic line shape of the coalescence point [$\tau \simeq 2\pi(^2\Delta)$] may be obtained with reasonable accuracy by inspection and used to calculate k_{ex} and k_{OH}. This is particularly useful if two resonances overlap or if the line shape in water is unusual. Strictly, the line shape at coalescence corresponds to this given rate only if the line width is very much less than $^2\Delta$, which is not the case. However, spectral simulations using appropriate $^2\Delta$ values show that even if the line width equals $^2\Delta$, the apparent exchange rate is reduced only by a factor of about 1.6, well within the accuracy of the experiment.

The base-catalyzed rate constant, k_{OH}, can be used to measure the retardation of exchange for a given proton in the protein in comparison to an unstructured (non-H-bonded) model peptide such as poly(DL-alanine) (Englander & Poulsen, 1969). At room temperature and a frequency of 75 MHz, the isotope shift technique is sensitive to retardations between 1- and (1×10^4)-fold compared with the exposed amide protons of PDLA. The upper limit is imposed by the concentration of OH^- ions to which a protein may reasonably be exposed.

Results

The incorporation of [^{13}C]carbonyl-labeled amino acids (alanine, glycine, lysine, proline, and phenylalanine) into M13 coat protein has been described previously (Henry et al., 1987). Twelve of these resonances have been assigned: alanine-1, glycine-3, proline-6, lysine-8, and phenylalanine-11 from the N-terminus and lysine-40, phenylalanine-42, lysine-43/44, phenylalanine-45, lysine-48, and alanine-49 from the C-terminus.

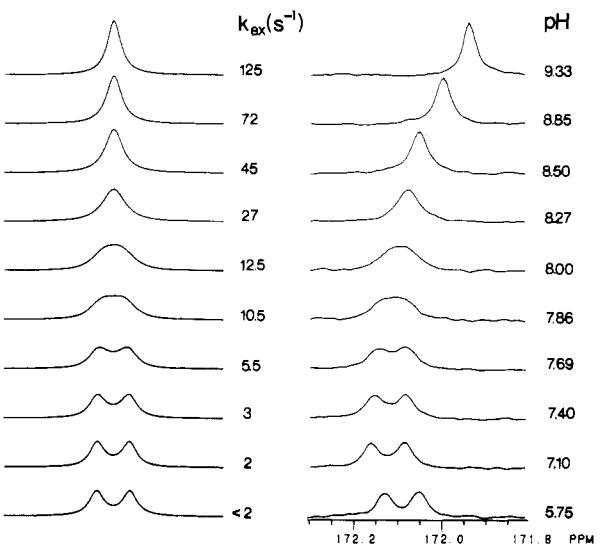

FIGURE 1: 75-MHz ^{13}C NMR spectra of the carbonyl carbon of glycine-3 (right) in equimolar H_2O/D_2O as a function of pH. To the left are simulated spectra from which the exchange rates of the adjacent amide proton (aspartic acid-4) were obtained. The protein concentration was 0.8 mM, and 5000 scans were collected. A line broadening of 1 Hz was used. The upfield shift at higher pH values is caused by deprotonation of the α-amino group of alanine-1.

The deuterium isotope shift on the carbonyl carbon is relatively small (6–7 Hz), and the method relies heavily on the narrow line width of the carbonyl carbon for resolution. For this reason, SDS was used to solubilize the protein as the line widths of many of the backbone carbonyl resonances in other detergents (such as deoxycholate or octyl glucoside) are much broader than would be expected from the known value of τ_c, the overall correlation time, suggesting aggregation or conformational heterogeneity (Henry et al., 1986; G. D. Henry, J. H. Weiner, and B. D. Sykes, unpublished data). The coat protein–SDS complex is a dimer which binds ~60 molecules of SDS under these conditions (Makino et al., 1975) and has an overall correlation time of about 10^{-8} s (Henry et al., 1986). The carbonyl carbons resonate in a region between 170 and 180 ppm downfield of Me_4Si. The exchange rates of the amide protons were determined from a series of pH titrations of the individually labeled proteins, and will be discussed in turn.

(*a*) *Glycine Label.* The glycine-3 resonance, reflecting exchange at aspartic acid-4, provides a good example of the application of the equilibrium isotope shift method to the measurement of exchange rates. Glycine-3 gives rise to one of the narrowest carbonyl resonances in the protein and is part of the short mobile region at the N-terminus of the protein [see Henry et al. (1987)]. The other three glycines, which reside in the hydrophobic region, resonate downfield of glycine-3 and have not been assigned. pH titration of C-1 glycine-labeled coat protein in 1:1 H_2O/D_2O results in a series of spectra characteristic of two-site exchange (Figure 1); the exchange rate is in the slow limit below pH 7.1 and in the fast limit above pH 9.3 with a coalescence pH between 8.0 and 8.3. Using a line width of 2.7 Hz (including 1-Hz line broadening) and a peak to peak separation of 6.0 Hz, we obtained the exchange rates, k_{ex} (also given in Figure 1), from curve fitting to the two-site exchange equation. Complete titration between the slow and fast limits occurs over 2 pH units, and the technique can be seen to be sensitive to values

Table I: Retardation of Exchange Rates of Amide Protons in M13 Coat Protein in Comparison with Poly(DL-alanine)

labeled residue	adjacent amide	coalescence pH at 23 °C	$t_{1/2}$ at pH 7.0 (s)	log k_{OH} (M^{-1} s^{-1})[a]	corrected log k_{OH} (M^{-1} s^{-1})[b]	retardation ($1/K_{op}$)[c]
Ala-1	Glu-2	6.05	0.0039	9.55	7.9	0.8
Gly-3	Asp-4	8.1	0.44	7.5/7.4*	7.1	4
Pro-6	Ala-7	8.2	0.69	7.3	7.3	4
Lys-8	Ala-9	8.7	2.19	6.8	6.5	16
Phe-11	Asp-12	8.9	2.76	6.7	6.5	16
Lys-40	Leu-41	~12	4383	3.5	3.2	31500
Phe-42	Lys-43	11.0	438	4.5/4.0*	4.3	2500
Lys-43	Lys-44	10.5	138	5.0	4.6	1250
Lys-44	Phe-45	10.5	138	5.0	5.0	500
Phe-45	Thr-46	9.7	17.44	5.9	5.3	250
Lys-48	Ala-49	8.0	0.438	7.5/7.8*	7.2	3
Ala-49	Ser-50	8.7	2.19	6.8	7.65	1

[a] Values indicated with an asterisk were determined from the slopes in Figure 6. [b] log k_{OH} values were adjusted for primary sequence effects according to values calculated from model peptides by Molday et al. (1972) (see text). [c] Retardations with respect to poly(DL-alanine), calculated from the corrected k_{OH} values. A k_{OH} value of 5×10^7 M^{-1} s^{-1} was used for poly(DL-alanine) determined from the data of Englander and Poulsen (1969) and adjusted to 23 °C by using their activation energy value of 73.15 kJ mol^{-1}.

of k_{ex} between 2 and 125 s^{-1} ($\tau \simeq 0.25$–0.004 s). The rate of exchange at coalescence (where the peak no longer has a flat-topped appearance) is between 12.5 and 27 s^{-1}. This is fully consistent with the predicted value of 20 s^{-1}). The chemical shift of glycine-3 is sensitive to the protonation state of the α-amino group of alanine-1 ($pK_a = 8.8$). This results in an upfield shift over the latter part of the pH titration which should not affect the exchange rate in any way.

The base-catalyzed rate constant k_{OH} can be obtained from the coalescence point ($1/\tau = k_{OH}[OH^-]_{measured}$) or more accurately from a plot of $-\log \tau$ vs. $pH_{measured}$, according to eq 3 (Figure 6). The slope of this plot is 0.97, close to the predicted value of 1.0 which is obtained with model peptides and many individual protons in proteins. The k_{OH} values of aspartic acid-4 and other protons are summarized in Table I. Amide exchange rates in proteins are not independent of primary sequence; however, except in unusual circumstances, these effects are reasonably small (<10-fold) [discussed by Englander and Kallenbach (1984)]. Using a series of model peptides, Molday et al. (1972) showed primary sequence effects (which are largely inductive effects) to be of short range, depending only on the nature of the exchanging residue and the residue preceding it in the sequence (the exchanging residue and the labeled residue in our situation). These authors compiled a table of "correction factors" which relate the exchange rate of a residue in a given sequence with that of poly(DL-alanine) in order that sequence-independent retardations of exchange may be calculated. All of the k_{OH} values given in Table I were adjusted according to the Molday factors; with the exception of the terminal residues (discussed later), these were very small. The largest correction (excluding the terminal residues) was applied to phenylalanine-45, resulting in a "corrected" exchange rate 4 times slower than the measured value. All other corrections resulted in an exchange rate 1–2.5 times slower than the measured rate. The corrected k_{OH} value was used to measure retardation of exchange by comparison with the k_{OH} value obtained for the freely exposed (non-hydrogen-bonded) amide protons of poly(DL-alanine) (PDLA) Hvidt & Nielsen, 1966; Englander & Poulsen, 1969). The amide of aspartic acid-4 has an effective exchange rate 5-fold slower than PDLA.

(*b*) *Lysine Label.* Four of the five lysine residues (40, 43, 44, and 48) are clustered in the C-terminal region of the molecule; the exception is lysine-8 [see Figure 1 of Henry et al. (1987)]. These monitor exchange at alanine-9, leucine-41, lysine-44, phenylalanine-45, and alanine-49. pH titrations of spectra acquired in H_2O and 1:1 H_2O/D_2O are compared in Figure 2a,b. Lysines-43 and -44 appear as a single peak in

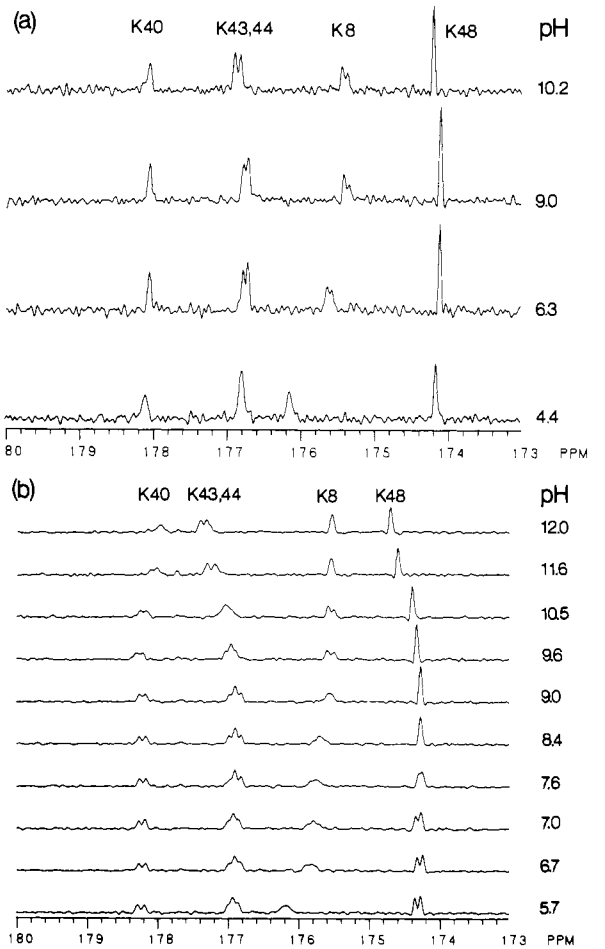

FIGURE 2: 75-MHz ^{13}C NMR spectra of the carbonyl region of [1-^{13}C]lysine-labeled coat protein (0.7 mM) in SDS as a function of pH. (a) 95% H_2O; (b) pH titration in 1:1 H_2O/D_2O showing coalescence of the isotopically shifted resonances at different pH values. In both (a) and (b), 5000 transients were averaged, and the free induction decay was weighted by multiplication with a double-exponential function to improve resolution.

95% H_2O at low pH values but are separated into two peaks at pH $\simeq$5. On the other hand, lysine-8 exists as a "doublet" in 95% H_2O over most of the range of the pH titration but is a single Lorentzian line at pH 4.0. The origin of the "double resonances" for certain amino acid residues in M13 coat protein will be the subject of a separate paper. The chemical shift changes of the lysine resonances with pH are small compared to their total dispersion, suggesting that no major conformational change occurs which involves the lysine resi-

dues over the pH range of the titration. A small downfield shift (0.5 ppm) of the lysine carbonyl carbon is observed in the model peptide Gly-Gly-Lys-Gly-Gly upon deprotonation of the ϵ-amino group (Keim et al., 1974). This probably accounts for the downfield shift observed at high pH for lysines-43, -44, and -48 in Figures 2 and 3.

The lysine label exhibits a wide range of amide exchange rates. Lysine-48, which like glycine-3 is one of the mobile terminal residues (Henry et al., 1987), reports exchange at alanine-49. The coalescence pH of approximately 8.0 (Table I) is only slightly higher than that expected for the freely exposed PDLA. A plot of $-\log \tau$ vs. $pH_{measured}$ for alanine-49 (Figure 6) is a straight line with a slope of 0.93, showing that eq 3 provides a satisfactory description of exchange in the OH^--catalyzed region. After small corrections for the Molday effects to k_{OH}, alanine-49 is only 3-fold retarded with respect to PDLA. At the other end of the scale, lysine-40 does not approach coalescence until pH 12, representing a (3.1×10^4)-fold retardation of leucine-41 over PDLA. pH measurements above 12 are not possible owing to the sodium sensitivity of the glass electrode. There are amide protons in M13 coat protein which exchange more slowly than leucine-41 (Cross & Opella, 1980; J. D. J. O'Neil and B. D. Sykes, unpublished results), but this degree of retardation represents the limit of the isotope exchange technique at room temperature. The other lysine residues reflect exchange rates which lie between these two extremes. The doublet character of lysine-8 in water (Figure 2) results in complex "triplet" in H_2O/D_2O mixtures due to resonance overlap. The triplet collapses to a doublet at about pH 9.0 and to a single Lorentzian line between pH 10.5 and 11.6. pH titration in H_2O (Figure 2) shows the lower pH transition to be collapse of the CONH and COND peaks due to exchange at alanine-9. In a similar way, lysines-43 and -44 yield a triplet in H_2O/D_2O due to the poor resolution of the individual resonance lines. These adjacent residues nevertheless appear to reflect similar rates of exchange, and the pH of coalescence for both was estimated to be 10.5, representing a retardation of approximately 1.2×10^3 for lysine-44 and 5×10^2 for phenylalanine-45, respectively. None of these resonances have line shapes suitable for determination of the exchange rate from computer simulations, and k_{OH} was determined from the coalescence pH.

(*c*) *Phenylalanine Label.* The three phenylalanine residues occur in both the N- and C-terminal regions. Near the N-terminus, phenylalanine-11 records exchange at aspartic acid-12 whereas in the C-terminal region two phenylalanine residues, phenylalanine-42 and phenylalanine-45 (reporting on exchange at lysine-43 and threonine-46, respectively), flank the pair of adjacent lysine residues. The ^{13}C NMR spectra of the labeled protein in 95% H_2O (Figure 3) show that phenylalanine-45 is a doublet like lysine-8; this persists until pH values above 12 are reached. This again results in a triplet composed of overlapping doublets when the protein is in 1:1 H_2O/D_2O. Phenylalanine-42 and phenylalanine-45 undergo small ($\simeq$0.5 ppm) downfield shifts at high pH, probably resulting from deprotonation of the adjacent lysine residues. Phenylalanine-11, in 50% H_2O/50% D_2O, coalesces at pH 8.9, giving a 16-fold retardation for aspartic acid-12 over PDLA, similar to alanine-9. Phenylalanine-45 and phenylalanine-42 coalesce at pH values of 9.7 and 11.0, respectively (Table I), representing retardations of 250 for threonine-46 and (2.5×10^3)-fold for lysine-43. Direct measurement of exchange rates is possible for both the phenylalanine-11 and phenylalanine-42 labels. The latter residue, which yields the exchange rates of

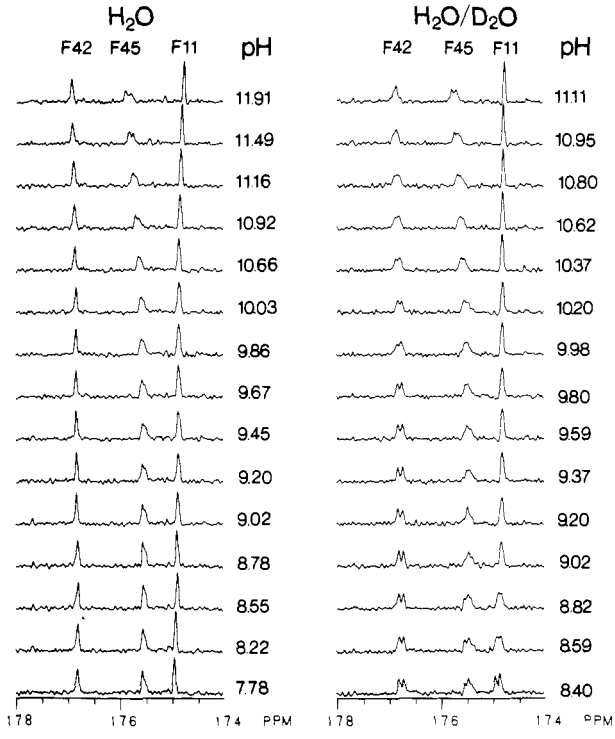

FIGURE 3: Carbonyl region of the 75-MHz ^{13}C NMR spectrum as a function of pH for SDS-solubilized coat protein labeled with [1-^{13}C]phenylalanine in (left) 95% H_2O and (right) 50% H_2O/50% D_2O. The protein concentration was 0.7 mM in each case, and the resolution was enhanced by weighting the free induction decay with a double-exponential function. 5000 transients were averaged.

lysine-43, gives a slope of 1.1 in a plot of $-\log \tau$ vs. $pH_{measured}$ (Figure 6) and allows k_{OH} to be calculated directly (Table I). At higher pH values (above 11.4), the exchange rate of lysine-43 becomes independent of pH. Aspartic acid-12, on the other hand, gives a slope of 2 in Figure 6, indicating that eq 3 does not apply. This could be due to a pH-dependent local conformational change involving aspartic acid-4 and resulting in a transition from a more slowly exchanging form to a more rapidly exchanging form. Other explanations are possible, however, and will be treated further in the discussion. Extrapolation of k_{OH} from the coalescence point relies on the relationship of eq 3; if the slope deviates from 1 during the pH titration, k_{OH} cannot be estimated reliably. If the deviation from unit slope represents a conformational change, then k_{OH} determined from the coalescence point will represent a weighted average of the k_{OH} values of the two forms.

(*d*) *Proline Label.* The single proline residue, proline-6, provides another example of peak splitting in H_2O (Figure 4a); this disappears above pH 11 and below pH 5. In 1:1 H_2O/D_2O (Figure 4b), typical CONH and COND peaks are observed at pH 4.3, but a triplet exists at higher pH values. The coalescence pH was judged to be $\simeq$8.2, resulting in an approximately 4-fold retardation for alanine-7 (Table I).

(*e*) *Alanine Label.* Of the 10 alanine residues, only alanine-1 and the penultimate residue, alanine-49, offer sufficient resolution for the determination of amide exchange rates. These two residues are of particular interest as they represent the terminal amides of the protein, glutamic acid-2 and serine-50; they also represent two of the more mobile residues in M13 coat protein (Henry et al., 1986a, 1987). The model compound experiments of Molday et al. (1972) show that the N- and C-terminal amides, unlike the rest, are subject to relatively large effects from the charged terminal groups. The N-terminal amide proton is more easily abstracted than it would be otherwise (due mainly to inductive effects) whereas

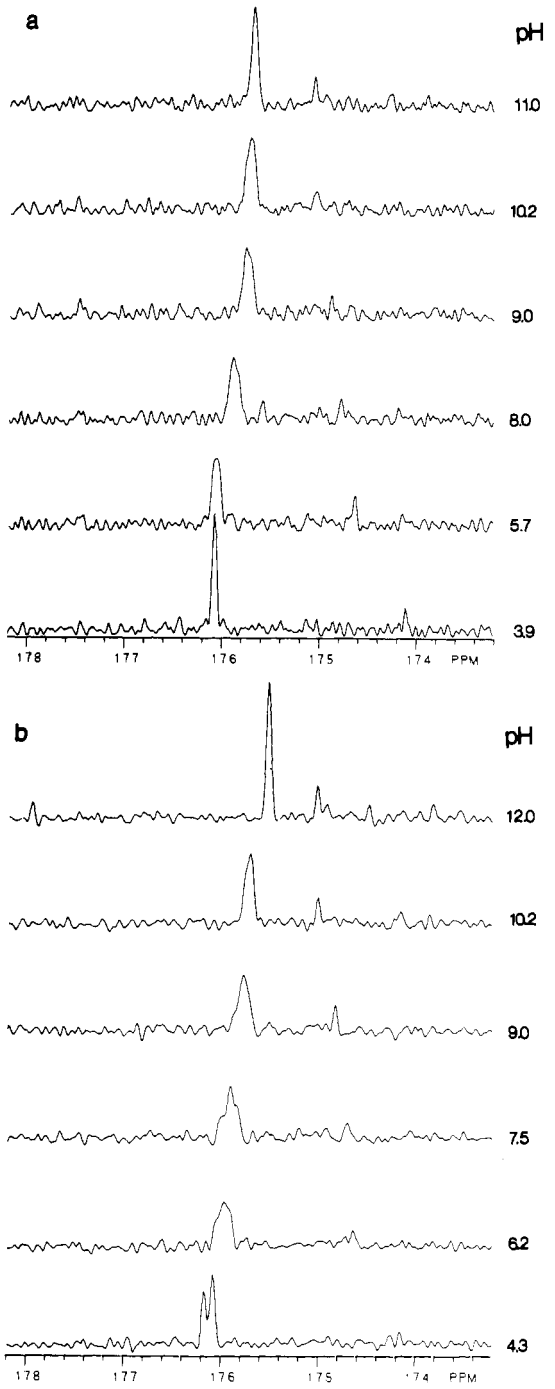

FIGURE 4: Carbonyl region of the 75-MHz ^{13}C NMR spectrum of [1-^{13}C]proline-labeled M13 coat protein in SDS micelles as a function of pH. (a) 90% H_2O; (b) 1:1 H_2O/D_2O. The protein concentration was 0.8 mM in both sets of spectra. 10000 transients were averaged. The minor upfield resonances probably arise from glutamic acid backbone carbonyls; glutamic acid is the major catabolite of proline.

the reverse is true for the C-terminal amide. This is demonstrated in Figure 5; a pH titration of C-1 alanine-labeled coat protein in H_2O is given in Figure 3 of Henry et al. (1987).

In 1:1 H_2O/D_2O, the alanine-1 resonances enter the exchange "window" at very low pH values. The coalescence pH was estimated to be 6.1, which is well below that which would be expected for PDLA (7.9). Above pH 7, the alanine-1 resonance begins to shift downfield and broaden considerably due to deprotonation of the N-terminal amino group (pK_a = 8.8). Alanine-49 (reflecting exchange at serine-50), on the other hand, exchanges 8 times more slowly than PDLA and 450 times more slowly than alanine-1 (reflecting exchange at glutamic acid-2); the coalescence pH was 8.7 (Table I).

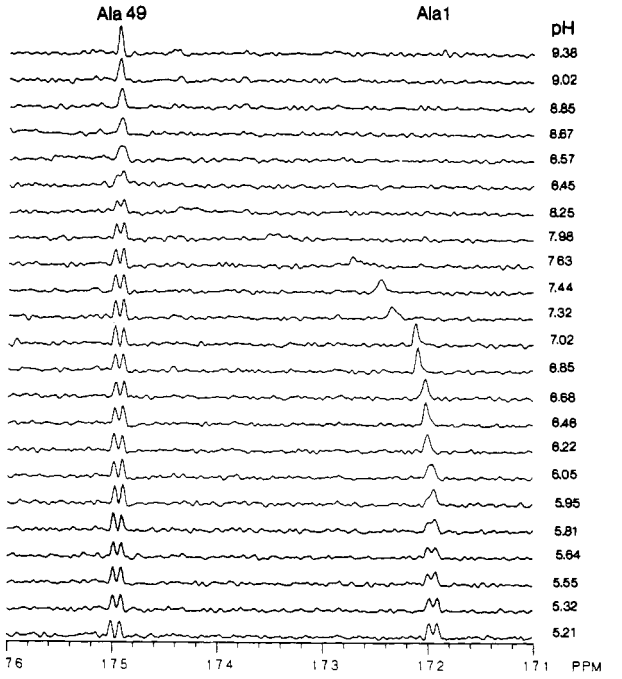

FIGURE 5: Carbonyl region of the 75-MHz ^{13}C NMR spectrum of [1-^{13}C]alanine-labeled coat protein solubilized in SDS and equimolar H_2O/D_2O as a function of pH. Only the region containing alanines-1 and -49 is shown. The protein concentration was 1.25 mM, and 5000 transients were averaged. Resolution was enhanced by weighting the free induction decay with a double exponential function.

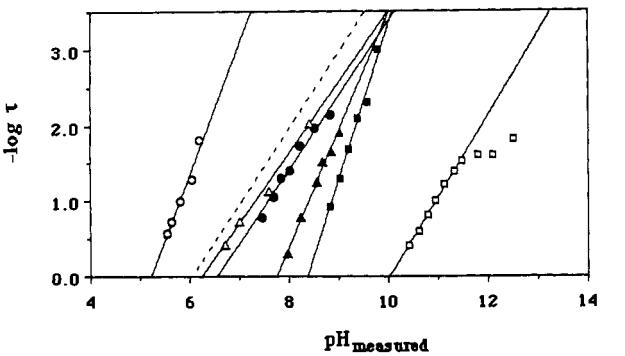

FIGURE 6: Plot of $-\log \tau$ vs. $pH_{measured}$ (see eq 3) for Glu-2 (○), slope = 1.73; Asp-4 (●), slope = 0.97; Asp-12 (■), slope = 2.04; Lys-43 (□), slope = 1.10; Ala-49 (△), slope = 0.93; and Ser-50 (▲), slope = 1.54. Poly(DL-alanine) (---), slope = 1.00, is included for comparison. k_{OH} is calculated from the intercept (intercept on the abscissa is 14 $-\log k_{OH}$). $pH_{measured}$ is p(H + D). No correction was made for deuterium isotope effects on the glass electrode, or the populations of protonated and deuteriated species. τ is equal to $1/2k_{ex}$. This graph is equivalent to the more conventional log k_{ex} vs. pH plots obtained from measurements made in a solvent composed of a single isotopic species where the relevent catalyst concentration is $[OH^-]_{measured}$ and not $[OH^-]_{measured}/2$.

Application of the Molday factors, however, leads to exchange rates for both glutamic acid-2 and serine-50 which are very similar to that of PDLA (actually retardations of 0.8 and 1, respectively), suggesting that the terminal amides exchange with the solvent as freely as unstructed model peptides. This is consistent with the high degree of backbone mobility at the extreme ends of the protein. However, the exchange rates of both glutamic acid-2 and serine-50 show a greater than unit dependence of $-\log \tau$ on $pH_{measured}$ (Figure 6) with slopes of 1.7 and 1.5, respectively.

Discussion

Use of the Equilibrium Isotope Shift Method To Measure Hydrogen-Exchange Rates. The deuterium isotope shift ob-

served for peptide carbonyl carbons in equimolar H_2O/D_2O was first applied to hydrogen-exchange measurements by Hawkes et al. (1978) for the peptide antibiotic viomycin, and the potential of the method for the measurement of rapid exchange rates was recognized by Kainosho and Tsuji (1982). It is similar, in principle, to the use of deuterium isotope shifts in equimolar H/D mixtures in the assignment of ^{13}C NMR spectra of sugars and other polyhydroxy compounds [see Reuben (1985) and references cited therein]. The isotope shift method is particularly well-suited to proteins such as M13 coat protein which have broad, unresolved amide proton spectra (Cross & Opella, 1980); the ^{13}C label provides resolution and facilitates assignment, and the narrow line width of the non-protonated carbonyl carbon allows resolution of the small two-bond isotope shift. The carbonyl carbon appears to be sensitive only to the following amide in the sequence; H-bonded deuterons exert a negligible effect. A small three-bond isotope shift ($\leq$2 Hz) on the carbonyl carbon, corresponding to deuteriation of the amide of the same residue, was observed by Hawkes et al. (1978) for viomycin, but the line widths in our experiment preclude such an observation. In principle, the same experiment should be possible with labeled α-carbons providing the line widths are sufficiently narrow. The major disadvantage of the method is that it can only be applied over a relatively narrow pH range.

Rapidly exchanging protons, which are most accessible to this and other equilibrium techniques [e.g., see Berger et al. (1959)], are the most difficult class to measure by the more usual "exchange-out" experiments which involve the time-dependent equilibration of a protonated protein with fully deuteriated solvent. The two types of measurement thus serve to complement each other. The exchange rates of side chain OH, SH, or NH_2 protons, which generally exchange more rapidly than backbone amide NH's, may also be determined from two-bond carbon–deuterium isotope shifts.

Analysis of Amide Exchange Rates. The mechanism of H exchange in proteins has been surrounded by much controversy centered about two opposing models (Woodward et al., 1982; Englander & Kallenbach, 1984). The solvent penetration scheme supposes that the catalyst (H^+ or OH^-) must diffuse through transiently forming channels in the protein toward the site of exchange. The local unfolding mechanism, by contrast, requires cooperative unfolding (i.e., H-bond breakage) of a small segment of polypeptide chain to precede the exchange event; exchange takes place in the unfolded form. These two models have proved very difficult to distinguish on kinetic grounds. We have adopted the local unfolding model, with its explicit dependence on H-bond breakage. This model is easier to quantitate and has been used very successfully recently, notably to explain H-exchange rates in the pancreatic trypsin inhibitor (Roder et al., 1985).

H exchange can be described by the following general equation for an individual hydrogen in a protein in equilibrium with H_2O and D_2O:

$$N(H) \underset{k_2}{\overset{k_1}{\rightleftharpoons}} O(H) \underset{k_3}{\overset{k_3}{\rightleftharpoons}} O(D) \underset{k_1}{\overset{k_2}{\rightleftharpoons}} N(D)$$

where N and O refer to the native and open forms, respectively. The rate constants for folding (k_2) and unfolding (k_1) in the protonated and deuteriated forms are taken to be the same. k_3 is the second-order rate constant for exchange in an exposed peptide and is most often the rate-limiting step. The exchange rate k_{ex} is (Hvidt & Nielsen, 1966)

$$k_{ex} = \frac{k_1 k_3[OH^-]}{k_1 + k_2 + k_3[OH^-]} \quad (4)$$

If $k_2 \gg k_1$ (i.e., the closed form is very much more stable than the open form), then this reduces to the more commonly used version (Englander & Kallenbach, 1984):

$$k_{ex} = \frac{k_1 k_3[OH^-]}{k_2 + k_3[OH^-]} \quad (5)$$

In the EX2 limit ($k_2 \gg k_3[OH^-]$) (Hvidt & Nielsen, 1966):

$$k_{ex} = \frac{k_1 k_3[OH^-]}{k_2} = K_{op} k_3[OH^-] = k_{OH}[OH^-] \quad (6)$$

where $K_{op} = k_1/k_2 = [O]/[N]$ and k_{OH} is from eq 2. The pH dependence of the exchange rates (Figure 6) shows that the EX2 limit applies here, except for lysine-43 at high pH. The retardation of exchange is thus equivalent to $1/K_{op}$, the inverse of the opening equilibrium constant (Roder et al., 1985). However, this does not apply to the most rapidly exchanging protons where the folded form may not be more stable than the unfolded form may not be more stable than the unfolded form and eq 5 rather than eq 6 is appropriate. In fact, the concept of a single opening equilibrium constant may be untenable under these conditions as these regions of the protein may be rapidly exchanging between a number of relatively unstable forms.

Model peptides such as poly(DL-alanine) and poly(DL-lysine) (Englander & Poulsen, 1969; Kim & Baldwin, 1982) obey eq 2 in the base-catalyzed regime. This is also true for many individual protons in proteins, but it is by no means universally the case (Richarz et al., 1979; Dempsey, 1986). It is probably unreasonable to expect proteins to conform precisely to model peptide standards as these do not account for the three-dimensional structure or pH-dependent conformational changes. Slopes greater than 1 in a plot of $-\log \tau$ vs. $pH_{measured}$ were observed for three out of the six protons which were measured: glutamic acid-2 (1.7), aspartic acid-12 (2.0), and serine-50 (1.5). This means that the retardation over PDLA is pH dependent and k_{OH} cannot be obtained exactly by extrapolation of the plots in Figure 6. Determination of the retardation rate from the coalescence point (Table I) is thus a compromise, but the effects should not be large enough to seriously distort our overall picture of the protein. Deviation of the $-\log \tau$ vs. $pH_{measured}$ slopes from unity to a value greater than 1 can be explained by additional catalysis of exchange or by pH-dependent conformational changes.

Charge effects, which are unlikely to be large at an ionic strength of 0.1 M (Kim & Baldwin, 1982), might shift the $-\log \tau$ vs. $pH_{measured}$ curve to the right or to the left (by increasing or reducing the local OH^- ion concentration), by they would be unlikely to alter the slope. A small pH-dependent conformational change is a plausible explanation for aspartic acid-12, but it is less easily invoked for glutamic acid-2 and serine-50, which are in the most highly mobile (i.e., least structured) regions of the protein. General acid or base catalysis by specific groups on the protein has been proposed by Dempsey (1986) to explain the pH dependence of several amides in apamin. A possible catalyst for the NH of glutamic acid-2 is its own carboxyl, which appears to ionize over the pH range of the experiment. The serine-50 NH may be similarly affected by the spatial proximity of the side chain hydroxyl. General acid/base catalysis is usually considered to be unimportant in proteins (Hvidt & Nielsen, 1966; Englander & Kallenbach, 1984) because added nucleophiles are ineffective catalysts of H exchange in small peptides (Molday et al., 1972). Nevertheless, the "effective" concentration of a protein side chain may be very high and could potentially

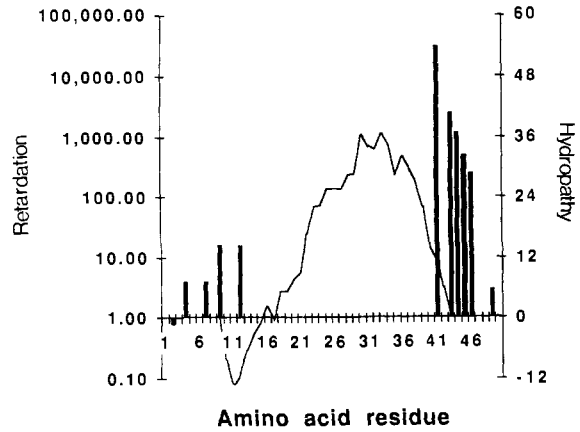

FIGURE 7: Retardation of exchange rates of amide protons of M13 coat protein [corrected for primary sequence effects according to Molday et al. (1972)] with respect to the unstructured peptide poly(DL-alanine) as a function of sequence (bars). Hydropathy (—), calculated according to Kyte and Doolitte (1981), is included to demonstrate the likely location of the membrane-spanning segment.

catalyze amide exchange. Such effects, which may be relatively small, would be averaged out unless individual amide protons are observed. As more individual amide exchange rates are determined, it may be necessary to reevaluate the potential of internal catalysis.

Amide Exchange Rates and Protein Structure. ^{13}C NMR relaxation experiments on M13 coat protein in SDS and deoxycholate micelles have demonstrated that only the extreme ends of the protein are undergoing spatial fluctuations on a time scale of less than 10^{-8} s (Henry et al., 1986). Approximately eight residues are particularly mobile, probably four from each end of the molecule (Cross & Opella, 1980; Henry et al., 1987). Unlike NMR relaxation measurements, H exchange can potentially identify and characterize motions which may be of large amplitude but occur on a relatively slow time scale. The retardation of exchange of the 12 assigned amides in M13 coat protein is summarized pictorially in a logarithmic plot in Figure 7; a hydropathy plot (Kyte & Doolittle, 1981) is included to show the likely location of the membrane-spanning segment. It can be seen that the more rapidly exchanging amides extend inwards beyond the first four residues at the N-terminus, including several residues which are rigid on a nanosecond time scale.

Amide exchange rates are now known for individual protons in several small proteins of known structure. The most thoroughly investigated of these is the basic pancreatic trypsin inhibitor, in which almost all of the amide protons are resolved and assigned and their exchange rates studied intensively under a wide variety of conditions (Hilton & Woodward, 1978; Wagner, 1983; Tuchsen & Woodward, 1985; Roder et al., 1985). Other proteins include the S-peptide of ribonuclease S (Kuwajima & Baldwin, 1983), apamin (Wemmer & Kallenbach, 1983; Dempsey, 1986), the *lac* repressor head piece (Boelens et al., 1985), and the terminal helix of cytochrome *c* (Wand et al., 1985). These proteins must serve as models for the interpretation of amide exchange data in M13 coat protein. Nevertheless, it should be remembered that these are generally small thermally stable proteins, three of which (the pancreatic trypsin inhibitor, ribonuclease, and apamin) contain disulfide bridges. They may not represent appropriate models for proteins in general, or for the small hydrophobic detergent-bound membrane protein.

All the exchange rates measured for the N-terminal region (up to and including aspartic acid-12) are relatively fast. As anticipated, the unstructured region at the extreme end shows very little retardation; however, the region between alanine-7 and aspartic acid-12 is retarded only 20-fold. Such values are significantly less than those calculated for helical regions in any of the proteins mentioned previously [summarized by Englander and Kallenbach (1984)], where retardations of at least 100-fold appear to be the rule. The short terminal helix of cytochrome *c* is retarded up to 10^7-fold (Wand et al., 1985). The relatively fast exchange rates in the coat protein suggest that this region of the protein backbone is in a state of dynamic flux, although on a time scale slower than that of the correlation time of the protein (10^{-8} s). It is probably folding and unfolding into one or more transiently stable configurations, although it is possible that some of these residues are non-H-bonded amides at the terminal end of a more stable helical region.

The more slowly exchanging amide protons detected in these experiments all arise from the C-terminal region. The mobile terminal residues (alanine-49 and serine-50) are retarded very little, but the exchange rate decreases progressively from 250-fold retardation (threonine-46) to (3.2×10^4)-fold retardation (leucine-41). This general pattern (see Figure 7) and a retardation of the order of 10^4 are together compatible with a helical structure by comparison with data from helices in other proteins. A simple model containing two strands of β-sheet would be expected to show an alternating pattern of retardation according to the alternate involvement in H bonding. A gradient in exchange rate is generally observed at the ends of α-helices due to independent local fraying (Kuwajima & Baldwin, 1983; Wand et al., 1985). It is possible that a helical segment extends from the C-terminal region throughout the membrane-spanning segment which is thought to extend from residue 21 to 39. Circular dichroism studies of the coat protein in SDS or deoxycholate micelles and phospholipid bilayers suggest it contains 50% α-helix and about 30% β-structure (Nozaki et al., 1978).

On the basis of relaxation experiments (Henry et al., 1986a), carbonyl line widths (Henry et al., 1987), and H-exchange results, we have devised a working model of the coat protein in SDS micelles comprising a helical hydrophobic segment which extends through most of the short C-terminal basic region and terminates in no more than four mobile (faster than 10^{-8} s) residues. The N-terminal region is of less well-defined structure, resulting in relatively rapid exchange rates although apart from the terminal four residues, this region is immobile on a 10^{-8} s time scale. Our model differs from that of Leo et al. (1987) derived for coat protein in phospholipid bilayers by solid-state ^{15}N NMR by ascribing more motion to the N-terminal region and less to the C-terminal region; under our conditions, phenylalanine-45 is immobile and exchanges relatively slowly. These differences may result from the nature of the environment or may merely reflect the different time scales involved in the two types of experiment.

ACKNOWLEDGMENTS

We thank Dr. Joe O'Neil for many discussions, Gerry McQuaid for upkeep of the spectrometer, and Dr. S. J. Opella for providing numerous preprints prior to publication and for many helpful discussions with him and the members of his research group.

Registry No. SDS, 151-21-3.

REFERENCES

Asbeck, V. F., Beyreuther, K., Kohler, H., von Wettstein, G., & Braunizer, G. (1969) *Hoppe-Seyler's Z. Physiol. Chem. 350*, 1047–1056.

Berger, A., Lowenstein, A., & Meiboom, S. (1959) *J. Am. Chem. Soc. 81*, 62–67.
Boelens, R., Gross, P., Scheek, R. M., Verpoorte, J. A., & Kaptein, R. (1985) *J. Biomol. Struct. Dyn. 3*, 269–280.
Cross, T. A., & Opella, S. J. (1980) *Biochem. Biophys. Res. Commun. 92*, 478–484.
Dempsey, C. E. (1986) *Biochemistry 25*, 3904–3911.
Englander, J. J., Calhoun, D. B., & Englander, S. W. (1979) *Anal. Biochem. 92*, 517–524.
Englander, S. W., & Poulsen, A. (1969) *Biopolymers 7*, 329–339.
Englander, S. W., & Kallenbach, N. R. (1984) *Q. Rev. Biophys. 19*, 521–655.
Feeney, J., Partington, P., & Roberts, G. C. K. (1974) *J. Magn. Reson. 13*, 268–274.
Hansen, P. E. (1983) *Annu. Rep. NMR Specrosc. 15*, 105–234.
Hawkes, G. E., Randal, E. W., Hull, W. E., Gattegno, D. & Conti, F. (1978) *Biochemistry 17*, 3986–3992.
Henry, G. D., Weiner, J. H., & Sykes, B. D. (1986a) *Biochemistry 25*, 590–598.
Henry, G. D., O'Neil, J. D. J., Weiner, J. H., & Sykes, B. D. (1986b) *Biophys. J. 49*, 329–331.
Henry, G. D., Weiner, J. H., & Sykes, B. D. (1987) *Biochemistry* (preceding paper in this issue).
Hilton, B. D., & Woodward, C. K. (1978) *Biochemistry 17*, 3325–3332.
Hvidt, A., & Nielsen, S. O. (1966) *Adv. Protein Chem. 21*, 287–386.
Kainosho, M., & Tsuji, T. (1982) *Biochemistry 21*, 6273–6279.
Keim, P., Vigna, R. A., Nigen, A. M., Morrow, J. S., & Gurd, F. R. N. (1974) *J. Biol. Chem. 249*, 4149–4165.
Kim, P. S., & Baldwin, R. L. (1982) *Biochemistry 21*, 1–5.
Kuwajima, K., & Baldwin, R. L. (1983a) *J. Mol. Biol. 169*, 299–322.
Kyte, J., & Doolittle, R. F. (1982) *J. Mol. Biol. 157*, 105–132.
Leo, G. C., Colagno, L. A., Valentine, K. G., & Opella, S. J. (1987) *Biochemistry 26*, 854–862.
Levitt, M. H., & Freeman, R. (1981) *J. Magn. Reson. 43*, 502–507.
Linderstrom-Lang, K. U. (1955) *Spec. Publ.—Chem. Soc. No. 2*, 1–20.
Linderstrom-Lang, K. U., & Schellman, J. A. (1959) *Enzymes, 2nd Ed. 1*, 443–510.
Makino, S., Woolford, J. L., Tanford, C., & Webster, R. (1975) *J. Biol. Chem. 250*, 4327–4337.
Marvin, D. A. (1966) *J. Mol. Biol. 15*, 8–17.
Marvin, D. A., & Wachtel, E. J. (1975) *Nature (London) 253*, 19–23.
McConnnell, H. M. (1958) *J. Chem. Phys. 28*, 430–431.
Molday, R. S., Englander, S. W., & Kallen, R. G. (1972) *Biochemistry 11*, 150–158.
Nakashima, Y., & Konigsberg, W. (1974) *J. Mol. Biol. 88*, 598–600.
Nozaki, Y., Chamberlain, B. K., Webster, R. E., & Tanford, C. (1976) *Nature (London) 259*, 335–337.
Nozaki, Y., Reynolds, J. A. & Tanford, C. (1978) *Biochemistry 17*, 1239–1246.
Reuben, J. (1985) *J. Am. Chem. Soc. 107*, 1756–1759.
Richarz, R., Sehr, P., Wagner, G., & Wuthrich, K. (1979) *J. Mol. Biol. 130*, 19–30.
Roder, H., Wagner, G., & Wuthrich, K. (1985) *Biochemistry 24*, 7396–7407.
Shindo, H., Egan, W., & Cohen, J. S. (1978) *J. Biol. Chem. 253*, 6751–6755.
Smilowitz, H., Carson, J., & Robbins, P. W. (1972) *J. Supramol. Struct. 1*, 8–18.
Strop, P., & Wuthrich, K. (1983) *J. Mol. Biol. 166*, 631–640.
Tuchsen, E., & Woodward, C. (1985) *J. Mol. Biol. 185*, 405–419.
Vasant Kumar, N., & Kallenbach, N. R. (1985) *Biochemistry 24*, 7658–7662.
Wagner, G. (1983) *Q. Rev. Biophys. 16*, 1–57.
Wagner, G., & Wuthrich, K. (1982a) *J. Mol. Biol. 155*, 347–366.
Wagner, G., & Wuthrich, K. (1982b) *J. Mol. Biol. 160*, 343–361.
Wagner, G., Stassinopoulou, C., & Wuthrich, K. (1984) *Eur. J. Biochem. 145*, 431–436.
Wand, A. J., Roder, H., & Englander, S. W. (1986) *Biochemistry 25*, 1107–1114.
Wemmer, D., & Kallenbach, N. R. (1983) *Biochemistry 22*, 1901–1906.
Woodward, C., Simon, I., & Tuchsen, E. (1982) *Mol. Cell. Biochem. 48*, 135–160.